8.4

TOWARDS THE RELATIONSHIP BETWEEN TOTAL LIGHTNING ACTIVITY AND DOWNWARD AS WELL AS UPWARD ICE MASS FLUXES IN THUNDERSTORMS

W. Deierling *[1] , W. A. Petersen [2] , J. Latham [3] , S. M. Ellis [3] and H. J. Christian Jr. [4]

[1] University of Alabama, Huntsville, Alabama
[2] Earth System Science Center, University of Alabama, Huntsville, Alabama
[3] National Center for Atmospheric Research, Boulder, Colorado
[4] Global Hydrology & Climate Center, NSSTC, Huntsville, Alabama

1. INTRODUCTION

This study focuses on the computation of precipitable and non precipitable ice mass, ice mass fluxes and the investigation of their relationship towards total lightning frequency. Microphysical as well as dynamical cloud processes contribute to thunderstorm electrification resulting in lightning. Generally a strong updraft within the mixed phase region is needed to produce sufficient electrification. In the mixed phase region non-inductive charge mechanisms take place that are thought to contribute mostly to thunderstorm electrification. In particular one of the most important non-inductive charge mechanisms include rimed graupel – ice interactions in the presence of supercooled liquid water (Saunders 1993). The charge transfer depends on temperature, liquid water content, particle size and impact velocity of the hydrometeors. Latham et al. 2004 suggests that significant charging is limited to an effective zone within an updraft. Following Latham et al. 2004 the upper limit of this charging zone is diffuse and located at the height where graupel will no longer be carried by the updraft speed w. The lower limit might characteristically be taken to be a few degrees colder than 0°C, dependent on the prevailing glaciation mechanism. The upper boundary limit is thought to typically lie between -15°C and -30°C.

Following these ideas analytical calculations from Petersen and Rutledge 2001 and Blyth et al. 2001 as well as computational results from Baker et al 1995 and 1999 yield the prediction that total lightning frequency F is roughly proportional to the product of the downward precipitation ice flux p and the upward flux of ice crystals I multiplied by some constant C:

$$F = C \cdot p \cdot I \ .$$

This prediction is currently lacking more definite support from field data. To this end, this study uses dual polarimetric radar data to derive bulk hydrometeor types (Vivekanandan et al. 1999), and mass contents of various particles (Straka et al. 2000) together with total lightning information to examine the flux hypothesis. Where possible three dimensional wind fields were calculated from dual Doppler radar data. It has to be kept in mind that radar reflectivity is dependent on the 6^{th} power of the particle diameter. Thus radar measurements are dominated by the largest particles in a given radar volume and will not resolve smaller ice crystals in the charging zone.

Results from two storms will be presented herein. Data from these storms originate from the Stratospheric-Tropospheric Experiment: Radiation, Aerosols and Ozone (STERAO) experiment that took place in the summer of 1996 in Northern Colorado and from the Severe Thunderstorm Electrification and Precipitation Study (STEPS) project which took place at the Colorado/Kansas border in the summer of 2000.

During STERAO polarimetric radar data were collected from the Colorado State University (CSU)-CHILL radar and total lightning activity was recorded by the Office Nationale d'Etudes et de Recherches Aerospatiales (ONERA) 3-D lightning interferometer as well as cloud-to-ground lightning by the National Lightning Detection Network (NLDN). These data were used to study the lifecycle of a severe storm observed on 10 July 1996. During STEPS, polarimetric radar data were collected from the CSU-CHILL radar as well as from the National Center for Atmospheric Research S-band dual-polarimetric Doppler weather radar (S-POL). Total lighting activity was recorded by the New Mexico Institute of Mining and Technology (NMIMT) deployable Lightning Mapping System (LMS) and cloud-to-ground

*Corresponding author address: Wiebke Deierling, Univ. Ala. Huntsville, Dept. Atmos. Science, 320 Sparkman Dr., Huntsville Al., 35805; email: deierling@nsstc.uah.edu

lightning data were available from NLDN. In this study a "garden variety" storm on July 6 2000 was analyzed.

2. METHOD

The NCAR particle identification algorithm (PID) was used to determine bulk hydrometeor types within thunderstorms from polarimetric radar data (Vivekanandan 1999) in radar coordinates. The NCAR PID is based on a fuzzy logic algorithm. It uses 9 input variables: the radar reflectivity, the differential reflectivity, the linear depolarization ratio, the correlation coefficient, the specific differential phase, a temperature profile, the standard deviation of velocity, the standard deviation of differential reflectivity and the standard deviation of the differential phase to distinguish between 17 output categories which are listed in Table 1.

Outputs
1. Cloud Drops
2. Drizzle
3. Light Rain
4. Moderate Rain
5. Heavy Rain
6. Hail
7. Hail/Rain mix
8. Graupel/Small Hail
9. Graupel/Small Hail/Rain mix
10. Dry Snow
11. Wet Snow
12. Irregular Ice Crystals
13.Horizontally Oriented Ice Crystals
14. Super Cooled Liquid Drops
15. Insects
16. Second Trip
17. Ground Clutter

Table 1: List of NCAR PID outputs.

Because of similarities in some of the hydrometeor classifications and because of microphysical reasons, two or more particle classifications were in some cases added together. In this study the hail, hail/rain mix, graupel/small hail and graupel/small hail/rain mix PID categories above the -5°C level were taken to represent precipitable ice in the charging zone over individual radar volumes. As mentioned in the introduction, ice crystals are not represented in the updraft region by the radar data. Therefore PID identified dry snow, irregular ice and oriented ice crystal categories above -50°C level were chosen to represent non precipitable ice.

To compute the mass of individual hydrometeor types, reflectivity (Z) – mass content (M) relationships of the kind $M = aZ^b$ were chosen from the literature that represent different thunderstorm ice types. The Z-M relationships for hail, graupel and thunderstorm anvil ice are given in table 2. Note, that Z is multiplied by a factor of 5.28 (Sassen 1987) to account for the lower dielectric constant for ice.

Hydro-meteor categories	**NCAR PID categories**	**Z-M relationship [g/m^3]**	**Reference**
Non precip ice	Dry snow, Oriented ice, Irregular ice	$M = 0.017 * Z^{0.529}$	Heymsfield and Palmer, 1986
Graupel	Graupel, Graupel/rain mixture	$M = 0.001 * Z^{0.712}$	Kajikawa and Kiba, 1978
Hail	Hail, Hail/rain mixture	$M = 0.00019 * Z^{0.67}$	Federer and Waldvolgel, 1975

Table 2. M-Z relationships for various hydrometeor types .

For each of the PID categories listed in table 2, individual ice mass contents were calculated for each radar gate in each plan position indicator (PPI) scan composing a radar volume. Also the volume of the individual radar gates of the individual PPI scans were computed in radar space and the mass contents were then divided by the radar volume for each radar gate. Finally the mass values were summed over the radar volume scan. Beam overlaps were identified and removed by applying the microphysical characteristics of the lower half of an overlapping area of two vertically stacked gates to the radar characteristics of the lower gate and the upper half area to the upper gate's characteristics. The center time of a volume scan was addressed to the volume.

During STEPS the S-Pol and CHILL radars were positioned to allow dual Doppler synthesis. Thus for the STEPS storm investigated in this paper a dual Doppler analyis was performed. First radar velocities were unfolded manually using the NCAR software soloii. Contamination such as second trip and ground clutter were removed using the PID information. In a second step, the NCAR Reorder software was used to convert the radar data from radar space onto a Cartesian grid. A Cressman filter weighting function was used for the

conversion and a grid spacing in x,y,z directions of 1 km with a radius of influence of 1.5 km was chosen in accordance with the mean 'width' of the radar gates for the lifetime of the storm. Finally the NCAR Custom Editing and Display of Reduced Information in Cartesian Space (CEDRIC) software was applied to determine a three dimensional wind field (u,v as the horizontal wind components and w as the vertical wind component). Vertical wind velocities were determined with three separate methods: integrating the mass continuity equation upward, downward and variationally. To relate the microphysics data to a 3D wind field on a Cartesian grid the PID output was gridded with the NCAR/ATD software package REORDER using a closest point weighting scheme. Temperature, reflectivity and radial velocity fields were gridded using a Cressman filter weighting scheme as mentioned above. To compute precipitable ice mass contents and ice mass the Z-M relationships (table 2) were applied to each radar grid similar to the procedure in radar space without the necessity of taking overlaps into account. Note that a comparison between total fractions, total mass content and total mass calculated in radar space and in Cartesian space was performed. When gridding the data smoothing of the radar variables inevitably occurs. The comparison (not shown) showed that this does not influence the trend of the time series of fractions, mass content or mass values.

For the 6 June 2000 case, only grids containing precipitable ice mass were multiplied with vertical velocities in the updraft region. The total value of these products were multiplied by the total of small ice mass above -50°C.

3. RESULTS

Results from two storms are presented in the following. The first storm occurred during the STERAO project on 10 July 1996. In the first part of its lifetime the storm exhibited multicellular character and transitioned into a low precipitation supercell in its later lifetime. The second storm occurred during the STEPS project on 6 June 2000 and is characterized as a 'garden variety' single cell storm.

In the following, first, for both storms the time series of total particle mass was overlaid with 1-minute total lightning activity. Additionally for the 6 June STEPS storm the product of precipitable ice mass and vertical updraft velocity was computed. The total value of these products was also multiplied by the total of small ice mass above -50°C and plotted.

3.1 STERAO 10 JULY STORM

The STERAO 10 July storm exhibited electric activity for 4.5 hours and had as mentioned above multicellular character with 2-4 cores oriented NW-SE along a confluence line in the first part of its life time from about 22:50 UTC to 1:20 UTC. In the second part of its lifetime, from approximately 1:20 until 2:30 UTC the storm had the characteristics of a low precipitation supercell displaying short lived low and mid level rotation, a bounded weak echo and a long lived updraft (Dye et al 2000). As can be seen in Figure 1 the first maximum in total lightning frequency occurred around 23:17 UTC with over 50 flashes per minute. Subsequent peaks of around 30 flashes per minute occurred and were associated with new cell development and cell mergers. During the supercell stage of the storm its total lightning frequency peaked around 57 flashes per minute. Note that this storm produced very little cloud-to-ground lightning (Lang et al, 2000; Dye et al, 2000; Defer et al, 2001). Defer et al. (2001) showed that fewer than 2% of the total flashes were cloud to ground over the lifetime of the storm.

Figure 1 shows total lighting frequency and totals of graupel/small hail and graupel/small hail/rain mixture mass as well as hail and hail/rain mixture mass trends above -5°C plotted against time. It can be seen that the trend of the graupel/small hail mass follows very well the trend of total lighting. This is also true for their mass content trends above -5°C. The hail mass trend as well as mass content trend above the -5°C level correlate fairly well with total lighting activity, however not quite as well as the graupel.

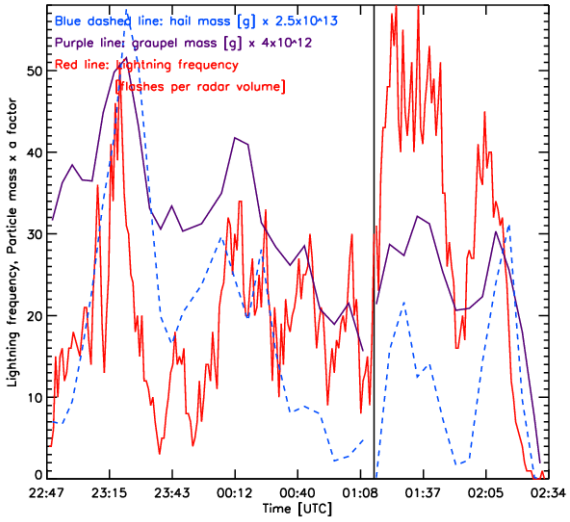

Figure 1. One minute lightning frequency (solid red line) and mass of larger hail and hail/ rain mixture above the -5°C level multiplied by a factor (blue dashed line) and the sum of small hail/graupel and small hail/graupel/rain mixture above the -5°C level multiplied by a factor (purple line). Left of the black line the 10 July storm was

of multicellular character, right of the black line of supercelluar character.

Figure 2 shows the total lighting frequency and precipitable ice mass above -5°C, non precipitable ice mass above the -50°C and the product of both. All trends correlate very well.

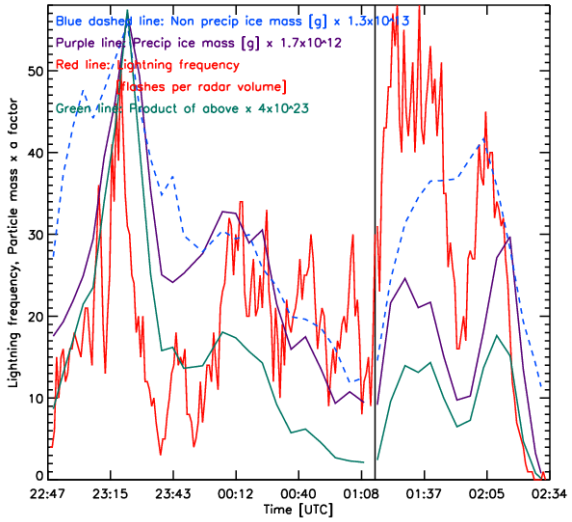

Figure 2. One minute lightning frequency (solid red line) and mass of precipitable ice above -5°C multiplied by a factor (purple line), the mass of non precipitable ice above the -50°C level multiplied by a factor (blue dashed line) and the product of both multiplied by a factor (green line).

3.2 STEPS 6 JUNE STORM

The STEPS 6 June storm had a lifetime of about 4 hours. It developed along a boundary that could be identified in the radar data. The 6 June STEPS storm is a good example of a garden variety single cell storm. Total lightning peaked around 22:20 UTC at approximately 25 flashes per minute, 30 minutes after its first flash was recorded and about an hour into its life time. The storm exhibited very few cloud to ground flashes that mostly occurred at the end of the storm's lifetime (not shown).

Figure 3 shows graupel/small hail mass trends and hail mass trends above the -5°C level similar to the STERAO case. Graupel mass as well as mass content trends (not shown) agree fairly well with the trend of total lightning. This is not the case for the time series of hail mass and hail mass contents. Similar to Figure 2, Figure 4 shows trends for precipitable ice mass above the -5°C level and non precipitable ice mass above the -50°C level. Non precipitable ice mass and ice mass content trends follow the trend of total lighting activity well. The same is true for precipitable ice masses and ice mass contents.

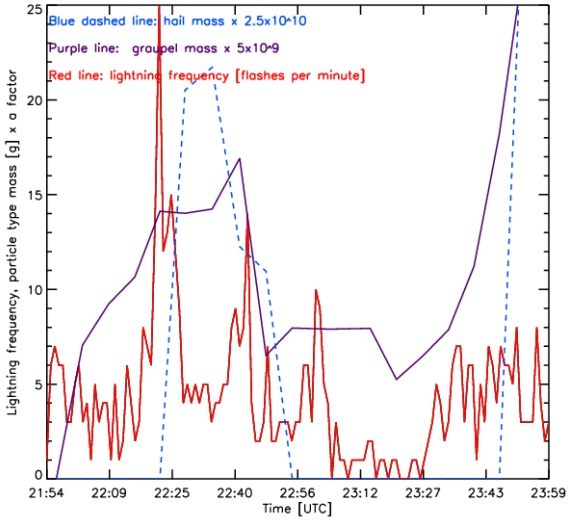

Figure 3. One minute lightning frequency (solid red line) and mass of larger hail and hail/ rain mixture above the -5°C level multiplied by a factor (blue dashed line) as well as the sum of small hail/graupel and small hail/graupel/rain mixture above the -5°C level multiplied by a factor (purple line).

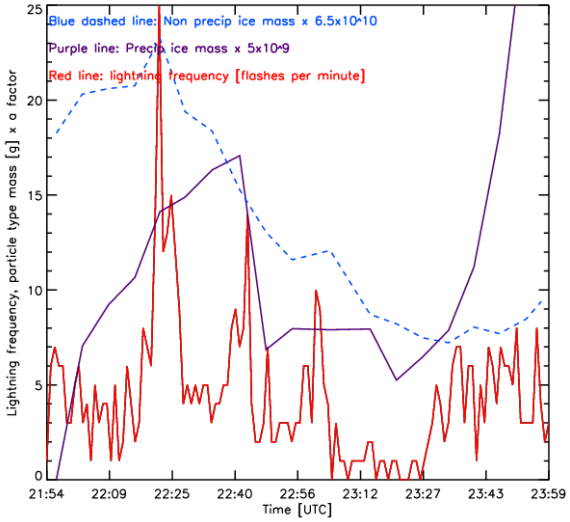

Figure 4. One minute lightning frequency (solid red line) and mass of precipitable ice above -5°C multiplied by a factor (purple line), the mass of non precipitable ice above the -50°C level multiplied by a factor (blue dashed line).

Finally Figure 5 shows the product of precipitable ice mass and vertical velocity as well as the product of precipitable ice mass, vertical velocity multiplied with the non precipitable ice mass. Again a good correlation between these trends and the trend of total lighting can be seen.

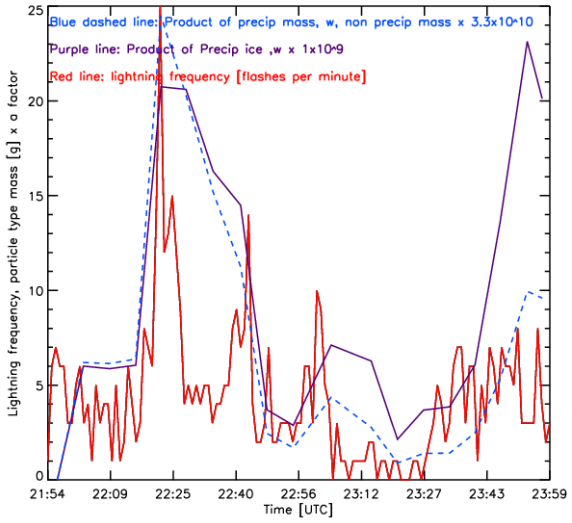

Figure 5. One minute lightning frequency (solid red line) and the product of mass of precipitable ice above -5°C and vertical updraft velocity w multiplied by a factor (purple line) and product of this times non precipitable ice mass above the -50°C level multiplied by a factor (blue dashed line).

5. CONCLUSIONS AND OUTLOOK

Overall bulk microphysical trends of precipitable ice mass and mass contents show a good relationship to total lightning activity in all cases. This is also true for non precipitable ice mass and mass content trends above the -50°C level as well as their products. Including vertical velocity values further improves the correlation, giving support for the flux hypothesis.

Future plans include computing a representative small ice flux as well as the product of non precipitable ice fluxes with precipitable ice fluxes for a number of storms.

6. ACKNOLEDGEMENTS

WAP and WD acknowledge funding from NASA ESE Lightning Imaging Sensor Project. JL wishes to acknowledge the support of USRA/NASA. The authors gratefully acknowledge Mr. David Brunkow and Mr. Patrick Kennedy for providing the CHILL radar data and Dr. Eric Defer for providing total lightning data for the STERAO 10 July storm.

7. REFERENCES

Baker, M.B., H.J. Christian and J. Latham, 1995: A computational study of the relationships linking lightning frequency and other thundercloud parameters. Q. J. R. Meteorol. Soc., **121**, 1525-1548.

Backer, M.B., A.M. Blyth, H.J. Christian, A.M. Gadian, J. Latham and K. Miller, 1999: Relationships between lightning activity and various thundercloud parameters: satellite and modelling studies. Atmos. Res., **51**, 221-236.

Blyth, A.M., H.J. Christian, K. Driscoll, A.M. Gadian and J. Latham, 2001: Determination of ice precipitation rates and thunderstorm anvil ice contents from satellite observations of lightning. Atmos. Res., **59-60**, 217-229.

Defer, E. P. Blanchet, C. Thery, P. Laroche, J.E. Dye, M. Venticinque, K.L. Cummins, 2001: Lightning activity for the 10 July, 1996, storm during the Stratosphere-Troposphere Experiment: Radiation, Aerosol, and Ozone-A (STERAO-A) experiment. J. Geophys. Res., **106**, 10,151-10,172.

Dye, J.E., Ridley, BA, Skamarock W., Barth, M., Venticinque, M., Defer, E, Blanchet, P., Thery, C., Laroche, P., Baumann, K., Hubler, G., Parrish, D.D., Ryerson, T., Trainer, M., Frost, G., Halloway, J.S., Matejka, T., Bartels, D., Fehsenfeld, F.C. Tuck, A., Rutledge, S.A., Lang, T., Stith, J., Zerr, R., 2000. An overview of the Stratospheric-Tropospheric Experiment: Radiation, Aerosols, and Ozone (STERAO)-Deep Convection experiment with results for the July 10, 1996 storm. J. Geophys Res., **105**, 10,023-10,045.

Federer, B. and A. Waldvogel, 1975: Hail and Raindrop Size Distributions from a Swiss Multicell Storm. J. Appl. Meteor., **14**, 91-97.

Heymsfield, A.J., and A.G. Palmer, 1986: Relations for deriving thunderstorm anvil mass of CCOPE storm water budget estimates. J. Climate Appl. Meteor., **25**, 691-702.

Kajikawa, M. and K. Kiba, 1978: Observation of the size distribution of graupel particles. Tenki. **25**, 390-398.

Lang, T.J., S.A. Rutledge, J.E. Dye, M. Venticinque, P. Laroche and E. Defer, 2000: Anomalously low negative cloud-to-ground lightning flash rates in intense convective storms observed during STERAO-A. Mon. Wea. Rev.,**128**,160-173.

Latham, J. A.M. Blyth, H.J. Christian Jr., W. Deierling and A.M. Gadian, 2004: Determination of precipitation rates and yields from lightning measurements. Journal of Hydrology, **288**, 13-19.

Petersen, W.A. and S.A. Rutledge, 2001: Regional Variability in Tropical Convection: Observations from TRMM. J. Climate, **14**, 3566-3586.

Sassen, K., 1987: Ice Cloud Content from Radar Reflectivity. J. of Climate and Appl. Meteor., **26**, 1050-1053.

Saunders , C. P. R., 1993 : A Review of Thunderstorm Electrification Processes. J. Appl. Meteor., **32**, 642-655.

Straka J.M., D.S. Zrnic, A.V. Ryshkov, 2000: Bulk hydrometeor classification and quantification using polarimetric radar data: synthesis of relations. J. Appl. Meteor.,**39**, 1341-1372.

Vivekanandan, J., D.S. Zrnic, S. M. Ellis, R. Oye, A. V. Ryzhkov, and J. Straka, 1999: Cloud microphysics retrieval using S-band dual-polarization radar measurements. Bull. Amer. Meteor. Soc., **80**, 381-388.